ELSEVIER

Polymer 42 (2001) 2941–2946

polymer

www.elsevier.nl/locate/polymer

SANS study of multilayer nanoparticles based on block copolymer micelles

J. Pleštil[a,*], H. Pospíšil[a], P. Kadlec[a], Z. Tuzar[a], J. Kříž[a], V.I. Gordeliy[b]

[a]*Institute of Macromolecular Chemistry, Academy of Sciences of the Czech Republic, Heyrovsky Sq. 2, 162 06 Prague 6, Czech Republic*
[b]*Frank Laboratory of Neutron Physics, Joint Institute for Nuclear Research, 141980 Dubna, Moscow Region, Russia*

Received 26 June 2000; received in revised form 2 August 2000; accepted 30 August 2000

Abstract

A novel type of three-layer nanoparticles was studied using small-angle neutron scattering (SANS). The particles were prepared by adding methyl methacrylate monomer to a polystyrene-*block*-poly(methacrylic acid) micellar solution in aqueous buffer and subsequent polymerization by γ-irradiation. The contrast-matching SANS experiments revealed that upon polymerization, the PMMA chains form a layer on the surface of the PS cores of the original micelles. This is in agreement with the finding that at room temperature, MMA monomer molecules do not penetrate into the micelle core in detectable amounts. In the presented example, the mean core radius of original micelles and the layer thickness were determined to be 99 and 17 Å, respectively. Both characteristics are expected to be controllable by the choice of block copolymer micelles and the parameters of the polymerization process.

Keywords: Small-angle neutron scattering; Multilayer nanoparticles; Coated micellar cores

1. Introduction

Block copolymer micelles are polymolecular particles with a dense core formed by insoluble blocks and a protective corona formed by swollen soluble blocks (for recent reviews, see, e.g. Refs. [1,2]). Most potential applications of micelles are based on uptake and/or release of sparingly soluble compounds into and from micellar cores. It is desirable to have a possibility of controlling this process by variation of micelle parameters. Promising candidates for such purpose are onion-type micelles. Unlike the commonly studied two-component core/corona micelles, onion-type micelles have a concentric three-layer structure. The simplest way to prepare three-layer micelles is to use an ABC triblock copolymer. Kříž et al. [3] prepared such micelles from the poly(2-ethylhexyl acrylate)-*block*-poly(methyl methacrylate)-*block*-poly(acrylic acid) copolymer in D_2O. In their study utilizing several different techniques, the first attempt to characterize an onion-type micelle by means of small-angle neutron scattering (SANS) is reported.

Procházka et al. [4] developed a procedure for the preparation of multilayer micelles using two diblock copolymers of types AB and BC. In Ref. [5], this procedure was used to prepare onion-type micelles from polystyrene-*block*-poly(2-vinylpyridine)- and poly(2-vinylpyridine)-*block*-poly(ethylene oxide) copolymers. Interpretation of SANS data for such a system is not straightforward. In addition to the onion-like particles, a significant number of micelles is present formed by the stabilizing copolymer [5]. Therefore, we prepared quite analogous onion-type micelles from an ABC triblock copolymer, polystyrene-*block*-poly(2-vinylpyridine)-*block*-poly(ethylene oxide) (PS-*b*-PVP-*b*-PEO), in D_2O medium [6]. In this case, the PVP middle block is pH-sensitive, and, consequently, it is possible to control to some extent transport of solubilizate to or from the micelle core.

Another possible technique of preparing multilayer nanoparticles is polymerization of a suitable monomer in various domains of already prepared polymer micelles. Radiation [7] as well as peroxide-initiated [8] polymerization of a monomer swollen in the micellar core has been reported. In these cases, however, the formation of separate polymer layers in the micelle has not been considered.

Liu et al. [9] reported the results of a light scattering study of polymerization with block copolymers as dispersants. The authors extensively investigated the influence of various factors on the polymerization process. The light scattering techniques, however, could not provide direct information on structural details of the resulting particles.

* Corresponding author. Fax: +420-2-367-981.
E-mail address: plestil@imc.cas.cz (J. Pleštil).

0032-3861/01/$ - see front matter
PII: S0032-3861(00)00651-0

Recently, we prepared three-layer nanoparticles by solubilizing methyl methacrylate monomer in micellar solution and subsequent polymerization. In a separate paper, we report on the results of the NMR study aimed at elucidation of distribution of the monomer in micelles and its evolution during polymerization [10]. High-resolution NMR data also point to the conclusion that poly(methyl methacrylate) is formed at the micellar core–shell interface, but as the signal of the polymer cannot be detected, no direct proof could be obtained. The objective of the present paper is thus to characterize the structure of the novel type of three-layer spherical nanoparticles using the SANS technique.

2. Experimental

2.1. Preparation of samples

The micellar solution of polystyrene-*block*-poly(methacrylic acid) (PS-*b*-PMA≡SA) ($M_W = 42 \times 10^3$ g/mol, weight fraction of PS = 0.58) in 0.1 M aqueous borax was prepared by a procedure described earlier [11]. A part of the solution was transferred into 0.1 M borax in D_2O by dialysis. The copolymer concentrations were 1.69×10^{-3} and 1.92×10^{-3} g/ml in H_2O and D_2O borax solutions, respectively. MMA was added to the micellar solution in an amount comparable with that of the copolymer (volume fraction of MMA = 1.6×10^{-3}). The solutions were stored for one day and then the MMA was polymerized by γ-radiation (dose 2 kGy) at 295 K.

2.2. SANS measurements

SANS measurements were performed using the time-of-flight small-angle neutron spectrometer YuMO [12] at the IBR-2 pulsed reactor in the Joint Institute for Nuclear Research, Dubna, Russia. The solution was placed in an optical quartz cell with a path length of 2 mm. Scattering intensities were measured using an eight-ring detector. All measurements were corrected for background scattering. The correction for the wavelength dependent neutron transmission of the samples and for the detector efficiency, as well as absolute normalization, were performed employing a procedure based on the use of a vanadium standard, as described in Ref. [13]. Scattering data are presented as a function of the magnitude of the scattering vector, $q = (4\pi/\lambda)\sin\Theta$, where λ is the wavelength and 2Θ is the scattering angle. The SANS curves measured at two sample–detector distances differing by a factor of two did not exhibit any systematic deviation in the overlap q-range. The data taken from the individual detector rings coincide within statistical errors. The wavelength contribution to the q-resolution of this TOF spectrometer is negligible in comparison with the angular one [12]. These facts indicate that the principal parts of the SANS curves of the samples studied are not affected significantly by instrumental distortions.

2.3. Analysis of the SANS data

The theoretical scattering function of spherical particles having the Schulz–Zimm size distribution was fitted to the experimental SANS data within a properly chosen q-range (bare-core approximation [14], hereinafter BCA). Only the middle part of the SANS curve is taken into consideration in this approach. The innermost part, where the scattering from the whole micelle is observed, as well as the high-q part, where the scattering from the corona-forming single chains predominates, was disregarded in the fitting process. Though the BCA is not a universal approach, it can simply provide useful information for a wide class of micellar systems. The fit provides the mean radius of micellar cores, R_{core}, and the relative standard deviation, $\sigma/R_{core} = 1/\sqrt{(Z+1)}$, where Z is the width parameter of the Schulz–Zimm distribution. Other characteristics of the micellar cores (volume, aggregation number and mass) can be calculated using the n-th moment of the Schulz–Zimm distribution

$$\langle R^n \rangle = \left(\frac{R_0}{Z+1}\right)^n \frac{\Gamma(Z+n+1)}{\Gamma(Z+1)} \tag{1}$$

The core volume V_{core} will be presented as a mean value defined as

$$V_{core} \equiv \frac{\langle V^2 \rangle}{\langle V \rangle} = \frac{4\pi}{3}\frac{\langle R^6 \rangle}{\langle R^3 \rangle} \tag{2}$$

The mass of a particle derived from such a mean volume is then the same weight average as provided by zero-angle scattering intensities.

From V_{core}, the molar mass of the core, M_{core}, is calculated as

$$M_{core} = V_{core} d N_A \tag{3}$$

where d is the density of the core and N_A is Avogadro's constant. This way of determining M_{core} relies solely on the shape of the SANS curve. No information on the copolymer concentration and contrast factor is necessary.

The molar mass of the core can also be determined from the absolute scattering intensity extrapolated to vanishing q. The relevant relation reads

$$M_{core} = I_{core}(0) N_A / c_{core} (\Delta b_{core})^2 \tag{4}$$

where Δb_{core} and c_{core} are, respectively, the excess scattering amplitude (in cm/g) and the concentration (in g/cm^3) of the core-forming polymer. The extrapolated intensity, $I_{core}(0)$, can be calculated using the theoretical scattering curve in the BCA fitted to the experimental data within a properly chosen q-range.

In the case of simple micelles we employed the Pedersen and Gerstenberg model (hereinafter P and G) consisting of a spherical core and attached Gaussian chains [15]. This approach also provides information on the micelle corona, though, due to a larger number of fitting parameters, its application is not always straightforward. Specifically, it is

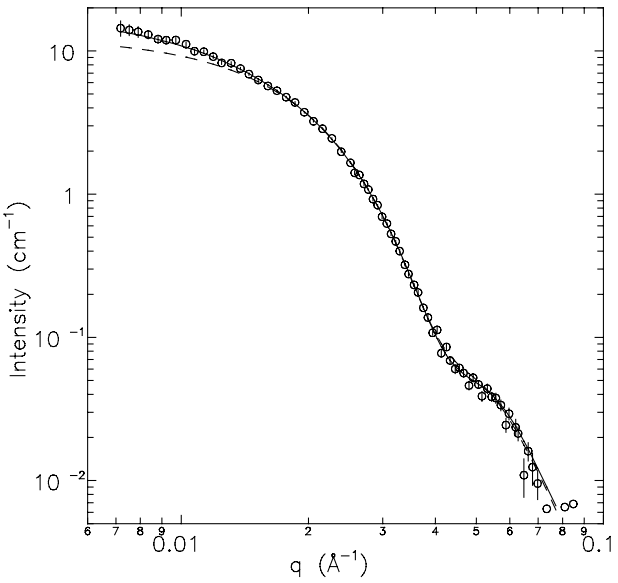

Fig. 1. SANS curve of PS-*b*-PMA in 0.1 M borax in D_2O ($c = 1.92 \times 10^{-3}$ g/ml) : experimental points with error bars (○), fitted scattering curves of the cores (dashed line, BCA) and the micelles (solid line, P and G model).

usually not possible to obtain a unique set of fitting parameters if the relative excess scattering amplitudes cannot be fixed. Analytical scattering functions for both approaches are given in Ref. [14].

3. Results and discussion

PS-*b*-PMA copolymers in aqueous media assemble to micelles with the PS core and PMA corona. The PS cores form nanosized hydrophobic domains in aqueous media, which attract nonpolar solutes, as demonstrated, e.g. in Ref. [16]. We expected that the added hydrophobic monomer would also concentrate within the micelles. Polymerization of the monomers then may lead to nanoparticles with a more complex structure than that of the original micelles.

We studied particles prepared by solubilization of methyl methacrylate in a PS-*b*-PMA micellar solution and subsequent polymerization. To take advantage of contrast variation, both the normal (hydrogenous) and deuterated homologs of the solvent (H_2O, D_2O) and monomer (h-MMA, d-MMA) were used. Besides the resulting particles, the original micelles as well as the micelles with solubilized monomer were investigated. The studied systems are denoted as SA, SA/h-MMA, SA/h-PMMA, SA/d-MMA and SA/d-PMMA, where SA stands for the PS-*b*-PMA copolymer.

3.1. PS-b-PMA micelles

We started with characterization of the micelles. The SANS curve of the PS-*b*-PMA micelles (SA) is shown in Fig. 1. An attempt was made to fit the scattering function of the P and G model [15] adapted for polydisperse systems [14] to the experimental data. To obtain reasonable results, the excess scattering amplitudes of the copolymer blocks had to be fixed. The amplitudes were estimated using the molar masses of the copolymer blocks and the material characteristics as $\Delta B_{core} = -1850 \times 10^{-12}$cm (PS) and $\Delta B_{chain} = -470 \times 10^{-12}$cm ($PMA^-$ anion). The fit provided the following values of the parameters: mean radius of the micelle core $R_{core} = 98.2$ Å, relative standard deviation of the radii $\sigma/R_{core} = 0.184$, radius of gyration of the corona chains $R_{G,c} = 96$ Å, starting point of the chains $R_{start} = 150$ Å. The last parameter was artificially implemented by the authors of the model and does not reflect the real structure of a micelle. Moving the starting point from the distance R_{core} to R_{start} mimics the effect of non-penetration of the chains into the core [15]. Though the micellar concentration was rather low (1.9×10^{-3} g/ml), the determined characteristics of the corona chains could be underestimated due to the concentration effect. For the corona parameters obtained by fitting the P and G model, however, the sensitivity to this effect was reduced by fixing the contrast factors.

Due to the artificial nature of $R_{start,}$ it may be questionable to interpret $R_{G,c}$ as the radius of gyration of the corona chains. Nevertheless, its value (96 Å) looks quite reasonable if an expanded PMA chain with molar mass of 18×10^3 g/mol is considered. Our result is close to those obtained for solutions of PMA of comparable molar masses [17,18]. From the hydrodynamic radius determined by dynamic light scattering ($R_H = 400$ Å) and from the core radius ($R_{core} = 99$ Å) we estimate the corona thickness as 301 Å, a value compatible with the radius of gyration of the corona chains given above.

Our second approach is based on the BCA [14]. This simple approach is insensitive to the concentration effect because it does not take into consideration the innermost part of the scattering curve. Consequently, it does not provide any direct information about the micellar corona. Its usefulness lies in the fact that it can be used for determination of the core parameters also in the cases when the excess scattering amplitudes are not known. The particles investigated in the present paper are an example of such systems.

The core parameters are given in Table 1. Their values ($R_{core} = 98.9$ Å, $\sigma/R_{core} = 0.20$) are very close to those based on the P and G model. This justifies the use of the BCA approach to the studied micelles in D_2O. The core molar mass was calculated from the volume using Eq. (3) ($M_{core} = 4.0 \times 10^6$ g/mol) and from the extrapolated intensity $I_{core}(0)$ using Eq. (4) ($M_{core} = 3.4 \times 10^6$ g/mol). Agreement between these two values is fairly good. The smaller value obtained from $I_{core}(0)$ may be due to a possible loss of the copolymer mass (15 wt.%) during the preparation (dialysis, centrifugation). The weight and number averages of the aggregation number were estimated from the corresponding mean volumes to be $N_w = 165$ and $N_n = 120$.

Table 1
Characteristics of the particles in D_2O determined using the BCA of SANS curves

	R_{core} (Å)	σ/R_{core}	$10^{-6} \times V_{core}$ (Å^3)	$I_{core}(0)$ (cm^{-1})
SA	98.9	0.20	6.3	12.5
SA/h-MMA	100.7	0.20	6.6	13.8
SA/d-MMA	100.2	0.20	6.5	12.5
SA/h-PMMA	116.3	0.19	9.7	31.0
SA/d-PMMA[a]	93.3	0.22	5.7	10.0

[a] The BCA is not satisfactory for this system.

It can be seen from Fig. 1 that the fitted model curves describe the experimental data fairly well. Clearly, using the BCA one cannot describe correctly that part of the SANS curve that is affected by the scattering from the particle corona. A comparison of the model curves reveals that the micelle coronas significantly contribute to the inner part of the SANS curve only. This is due to a lower scattering contrast (see Table 2) and the larger size of the corona in comparison with the core. For particles with coated cores, the applicability of the BCA primarily depends on the contrasts of the individual components. For the particles prepared using hydrogenous monomers in D_2O, the BCA approach is expected to work even better than for simple micelles because the relative scattering power of the core is higher in the former case.

3.2. Particles with MMA and PMMA

The particles obtained by adding monomer to a micellar solution and those formed by polymerization of the monomer will now be characterized using the BCA approach. An example of the BCA fit can be found in Fig. 2. This approach in its simple form (homogeneous core assumed) is applicable if the difference in the scattering contrasts for the core components can be neglected. For hydrogenous polymers in a deuterated solvent, this condition is usually met. The use of the P and G model does not lead to reliable results for these particles because the relative excess scattering amplitudes of the core and corona are not known a priori.

Fig. 2 shows the SANS curves of the studied systems. It can be seen that the addition of MMA monomer to the micellar solution has only a minor influence on the scattering intensities. As this is true for both the normal and the deuterated monomer, we may conclude that the monomer did not penetrate into the micelle core significantly. The NMR results [10] suggest that MMA is located predominantly in the micelle coronas. As follows from the above given analysis, the scattering contribution of the micelle corona is rather small in the q-range covered by the present experiment. At the smallest angles, where the scattering contribution of the corona is detectable, the SANS intensities (not shown in Fig. 2) for the micelles with solubilized deuterated monomer (SA/d-MMA) in H_2O are slightly higher than those obtained for neat micelles (SA). This indicates an accumulation of the monomer within the micelle corona. More detailed information about the location of MMA would be accessible if SANS data in smaller scattering vectors were available.

The SANS curves taken after polymerization differ significantly from the one observed for the original micelles (Fig. 2). For the SA/d-PMMA system, a deviation from the SANS curve of the simple micelles is observed only at small qs, while at higher angles the curves coincide. On the other hand, the SANS curve of the SA/h-PMMA system deviates appreciably in the region of the secondary maximum also, which reflects the size of the scatterer. These findings indicate that the cores of the studied particles are formed by the PS core of the original micelle and PMMA deposited on the surface of the core.

Similar conclusions can be drawn on the basis of the structure parameters of the cores determined using the

Table 2
Neutron scattering densities of the relevant compounds

	$10^{-10} \times \rho$ (cm^{-2})
d-PMMA	7.01
D_2O	6.36
d-MMA	5.56
PMA^-	3.00
PS	1.43
h-PMMA	1.07
h-MMA	0.85
H_2O	−0.56

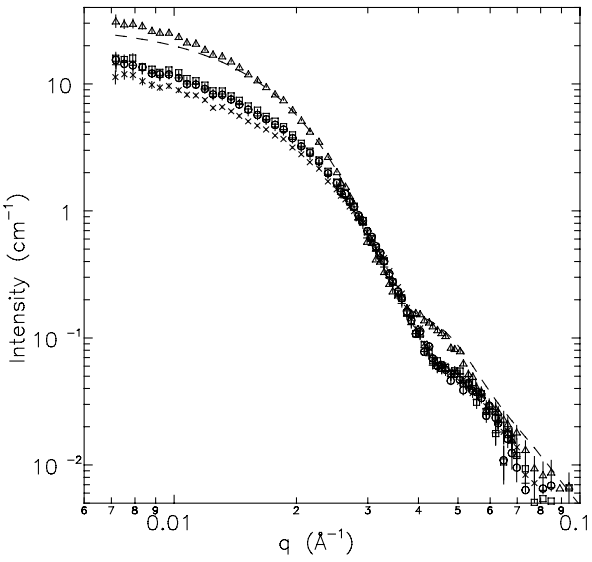

Fig. 2. Changes in the SANS curve of PS-*b*-PMA in 0.1 M borax in D_2O ($c = 1.92 \times 10^{-3}$ g/ml) induced by solubilization of methyl methacrylate monomer and subsequent polymerization (experimental points with error bars): (a) neat copolymer solution (○), (b) with h-MMA before (□) and after (△) polymerization, (c) with d-MMA before (+) and after (×) polymerization. The dashed line is an example of the BCA fit to SANS curves of the nanoparticles with coated cores.

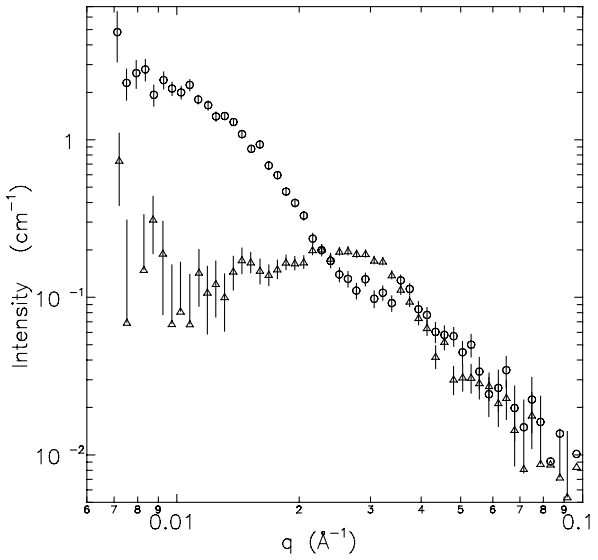

Fig. 3. SANS curves of PS-*b*-PMA with polymerized d-MMA in 0.1 M aqueous borax buffers at two contrasts: scattering length density of the solvent matches that of PS (○) and the mean scattering length density of the PS/d-PMMA core (△), respectively. The maximum at a non-zero q observed for the latter case indicates that the PS and d-PMMA components are separated.

BCA. Table 1 summarizes the results obtained for the particles in D_2O.The parameters are not sensitive to the presence of MMA. This means that the monomer does not swell the micelle core. Significant changes become apparent after polymerization.

Though the results obtained in H_2O (not shown in Table 1) are in qualitative agreement with the result for D_2O, they are less reliable because the approximations used (uniform scattering length density of core, neglected scattering from corona) are not as good as in D_2O. This can be seen from the scattering length densities given in Table 2. For example, the relative scattering contribution of the corona is much higher in H_2O than in D_2O.

Another evidence for the location of PMMA on the surface of PS cores can be provided by the variation of the contrast. We prepared SA/d-PMMA samples in two H_2O/D_2O mixtures chosen so as to match the scattering length density of PS and the mean scattering length density of the PS/d-PMMA core, respectively. The volume fraction of PS in the core (0.65) was estimated by comparing the core volumes for the SA and SA/h-PMMA in D_2O systems. It should be noted that in this solvent, the excess scattering densities of PS and h-PMMA are very close. Thus, the core parameters obtained using the BCA are close to their true values.

For a homogeneous core (mixture of PS and d-PMMA), the SANS curves under the contrast-matching condition of PS ($\rho = 1.43 \times 10^{10}\text{cm}^{-2}$) would reflect the overall size of the core while in the solvent with the scattering length density equal to that of the PS/d-PMMA core ($\rho = 3.3 \times 10^{10}\text{cm}^{-2}$), the scattering from the core would be suppressed. Fortuitously, under the latter conditions, the scattering from the PMA corona is also strongly suppressed (see Table 1).

Alternatively, if d-PMMA is separated from PS, the scattering is observable at both the contrasts. If the solvent is chosen to match the mean scattering length density of the core, then a SANS curve with main maximum at a non-zero q is expected.

The experimental scattering curves (Fig. 3) clearly suggest the second possibility, i.e. PMMA is separated from PS in the particle core. We have shown that MMA monomer does not penetrate into the PS cores. This suggests that PMMA chains are deposited on the surface of the PS cores. Further support for this conclusion is provided by comparison of the radius of gyration of d-PMMA domains obtained directly from the SANS curve using the Guinier approximation with that calculated from the core size distribution.

The Guinier approximation was applied to the scattering curve of SA/d-PMMA particles at negligible contrast for PS (circles in Fig. 3). Under this condition, the contrast of the PMA corona is also rather low and the main contribution to the observed scattering comes from the d-PMMA domains. We estimated the z-average of the radius of gyration of the PMMA domain as $R_{G,z} = 135(\pm 11)$ Å. Due to polydispersity, this value is larger than the mean outer radius of the PMMA shell (116 Å).

Let us now consider a homogeneous spherical shell with the inner and outer radii, γR and R, respectively. The z-average of the radius of gyration of such a shell can be calculated as

$$R_{G,z}^2 = \frac{3}{5}\frac{\langle R^8\rangle}{\langle R^6\rangle}\frac{(1-\gamma^5)}{(1-\gamma^3)} \tag{5}$$

where the n-th moment of the Schulz–Zimm distribution is given by Eq. (1) and γ has been defined implicitly.

Employing the core characteristics for the SA and SA/h-PMMA systems given in Table 1 ($Z = 28$, $R_0 = 116$ Å, $\gamma = 99/116 = 0.85$), we obtained using Eqs. (1) and (5) $R_{G,z} = 132$ Å. Thus, the model of the PS inner core with the PMMA shell leads to a value of the radius of gyration of the PMMA domain that is in good agreement with the value obtained directly from the SANS curve taken under proper contrast conditions.

4. Concluding remarks

Using the SANS technique, we have shown that polymerization of methyl methacrylate monomer solubilized in polystyrene-*block*-poly(methacrylic acid) micelles leads to formation of a PMMA layer on the surface of the PS core. In the presented example, the mean core radius was 99 Å and the layer thickness, 17 Å. The latter can be easily varied by variation of monomer concentration.

We expect that the structure of the resulting particles

would depend on many factors, primarily on the solubility of the monomer, oligomer and polymer, and on their interaction with the micelle components. Thus, the possibility of preparing particles with coated cores is to a great extent determined by the choice of the monomer–micelle pair. Nevertheless, for appropriate pairs, there still remain several factors enabling us to control the parameters of the particles (monomer concentration, details of polymerization procedure, duration of the solubilization process, repetition of the solubilization–polymerization process). Investigation of the influence of these factors on the structure of the resulting particles is under way.

Acknowledgements

The authors thank the Academy of Sciences of the Czech Republic (grant K2050602/12) and the Grant Agency of the Czech Republic (grants 203/97/249 and 203/00/1317) for financial support.

References

[1] Tuzar R, Kratochvíl P. In: Matijevic E, editor. Surface and colloid science, 15. New York: Plenum Press, 1993.
[2] Mortensen K. Curr Opin Colloid Interface Sci 1998; 3:12–19.
[3] Kříž J, Masař B, Pleštil J, Tuzar Z, Pospíšil H, Doskočilová D. Macromolecules 1998;31:41–51.
[4] Procházka K, Martin TJ, Webber SE, Munk P. Macromolecules 1996;29:6526–30.
[5] Pleštil J, Kříž J, Tuzar Z, Procházka K, Melnichenko YuB, Wignall GD, Talingting R, Munk P, Webber SE. Small-angle neutron scattering study of onion-type micelles. Macromol Chem Phys 2000 (in press).
[6] Pleštil J, Pospíšil H, Masar B, Kiselev MA. Annual Report 1998. FLNP, Joint Institute for Nuclear Research, Dubna, Russia, 1998. p. 63–6.
[7] Kříž J, Pleštil J, Tuzar Z, Pospíšil H, Brus J, Jakeš J, Masař B, Vlček P, Doskočilová D. Macromolecules 1999;32:397–410.
[8] Arca E, Cao T, Webber SE, Munk P. Polym Prepr (Am Chem Soc, Div Polym Chem) 1994;35(1):334–.
[9] Liu T, Schuch H, Gerst M, Chu B. Macromolecules 1999;32:6031–42.
[10] Kříž J, Kurková D, Kadlec P, Tuzar Z, Pleštil J. Macromolecules 2000;33:1978–85.
[11] Tuzar Z, Webber SE, Ramireddy C, Munk P. Polym Prepr (Am Chem Soc, Div Polym Chem) 1991;32(1):525–6.
[12] Ostanevich YuM. Makromol Chem, Macromol Symp 1986;15:91–103.
[13] Pleštil J, Ostanevich YuM, Bezzabotnov VYu, Hlavatá D. Polymer 1986;27:1241–6.
[14] Pleštil J. J Appl Crystallogr 2000;33:600–4.
[15] Pedersen JS, Gerstenberg MC. Macromolecules 1996;29:1363–5.
[16] Tian M, Arca E, Tuzar Z, Webber SE, Munk P. J Polym Sci, Part B: Polym Phys 1995;33:1713–22.
[17] Moan M, Wolff C, Cotton J-P, Ober R. J Polym Sci: Polym Symp 1977;61:1–8.
[18] Pleštil J, Ostanevich YuM, Bezzabotnov VYu, Hlavatá D, Labsky J. Polymer 1986;27:839–42.